Article

The Gas-Phase Acidity of 2(3H)-Oxepinone: A Step toward an Experimental Heat of Formation for the 2-Oxepinoxy Radical

Steven M. Kroner, Matthew P. DeMatteo, Christopher M. Hadad, and Barry K. Carpenter

J. Am. Chem. Soc., **2005**, 127 (20), 7466-7473• DOI: 10.1021/ja050173u • Publication Date (Web): 03 May 2005

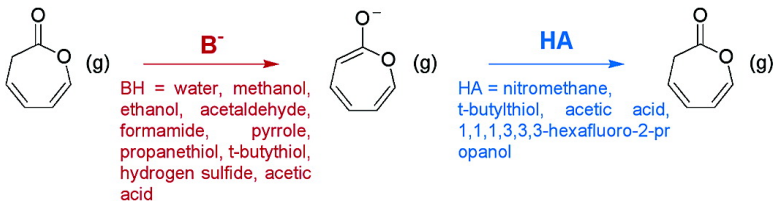

More About This Article

Additional resources and features associated with this article are available within the HTML version:

- Supporting Information
- Links to the 2 articles that cite this article, as of the time of this article download
- Access to high resolution figures
- Links to articles and content related to this article
- Copyright permission to reproduce figures and/or text from this article

View the Full Text HTML

J|A|C|S
ARTICLES
Published on Web 05/03/2005

The Gas-Phase Acidity of 2(3H)-Oxepinone: A Step toward an Experimental Heat of Formation for the 2-Oxepinoxy Radical

Steven M. Kroner,[†] Matthew P. DeMatteo,[‡] Christopher M. Hadad,*[,‡] and Barry K. Carpenter*[,†]

Contribution from the Department of Chemistry and Chemical Biology, Baker Laboratory, Cornell University, Ithaca, New York 14853, and Department of Chemistry, 100 West 18th Avenue, The Ohio State University, Columbus, Ohio 43210

Received January 11, 2005; E-mail: hadad.1@osu.edu; bkc1@cornell.edu

Abstract: In an effort to gain further insight into the oxidation of the phenyl radical, this contribution details the first of three experiments designed to establish the heat of formation of the 2-oxepinoxy radical. We report here the synthesis of the previously unknown 2(7H)-oxepinone (**12a**) and 2(3H)-oxepinone (**12b**). We have determined the gas-phase acidity ($\Delta_{acid}H_{298}$) of **12b** by means of a bracketing study employing a flowing afterglow apparatus with quadrupole mass spectrometric detection. In this experiment, compound **12b** was reacted in the gas phase with a series of bases of varying strength. A proton-transfer reaction was observed when **12b** was reacted with *t*-BuS$^-$, but not when **12b** was reacted with HS$^-$. We conclude that the gas-phase acidity of **12b** lies between those of *t*-BuSH and H_2S, and it is thereby assigned a value of $\Delta_{acid}H_{298} = 352 \pm 2$ kcal/mol. Additional support for this value was found by performing the reverse reactions (i.e. the 2-oxepinoxy anion (**15a**) was reacted with proton sources of differing acidities). Anion **15a** underwent a proton-transfer reaction with H_2S but not with *t*-BuSH, in agreement with the results from the forward reactions. The experimental value of the gas-phase acidity agrees well with those from DFT calculations, which predicted $\Delta_{acid}H_{298} = 348.9$ kcal/mol at the B3LYP/6-31+G(d) level and 349.2 kcal/mol at the B3LYP/aug-cc-pVTZ level.

I. Introduction

This report details the first of three experiments designed to establish the heat of formation of the 2-oxepinoxy radical, which is believed to be formed during the combustion of benzene. Benzene combustion routinely occurs within internal combustion engines. Although gasoline contains only a small amount of benzene, other aromatic species, such as toluene and ethylbenzene, comprise roughly 32% of the volume.[1] Like that of benzene, the combustion of these other aromatic species, apparently involves the formation and subsequent oxidation of the phenyl radical.[2−4] Even nonaromatic hydrocarbons can generate phenyl radical during combustion under fuel-rich conditions.[5] During combustion, the phenyl radical can lead to polycyclic aromatic hydrocarbons (PAHs), the building blocks of soot.[6−8] The presence of soot has been associated with a variety of medical, environmental, and mechanical problems.[9] Soot is a major component of urban smog[1] and apparently plays detrimental roles in atmospheric chemistry.[10] Thus, an understanding of the oxidative degradation of phenyl radical has potential economic and environmental value.

One of the first experiments to probe the benzene combustion mechanism was furnished by Fujii and Asaba, who observed CO and C_2H_2 as major decomposition products by shock tube pyrolysis methods.[11] Cyclopentadienyl radical (**5**) was also found to be a product of the combustion process.[12−14] Experiments that showed the presence of other intermediates, such as phenyl and phenoxy (**6**), suggested the following global mechanism:[3,14]

$$C_6H_6 + O_2 \rightarrow C_6H_5 + O_2H \quad (1)$$

$$C_6H_5 + O_2 \rightarrow C_6H_5O + O(^3P) \quad (2)$$

$$C_6H_5O \rightarrow C_5H_5 + CO \quad (3)$$

Generally, a mechanism can be supported by its ability to predict experimental observables, such as the prediction of the concentration of intermediates as a function of time throughout the course of a reaction. Within the benzene combustion mechanism, a model was built on the basis of experimental and

[†] Cornell University.
[‡] The Ohio State University.

(1) Sawyer, R. F. *Symp. (Int.) Combust., [Proc.] 24th* **1992**, 1423.
(2) Emdee, J. L.; Brezinsky, K.; Glassman, I. *J. Phys. Chem.* **1992**, *96*, 215.
(3) Brezinsky, K. *Prog. Energy Combust. Sci.* **1986**, *12*, 1.
(4) Wang, H.; Frenklach, M. *J. Phys. Chem.* **1994**, *98*, 11465.
(5) Marianov, N. M.; Pitz, W. J.; Westbrook, C. K.; Castaldi, M. J.; Senkan, S. M. *Combust. Sci. Technol.* **1996**, *116−117*, 211.
(6) Anon. *Gas Age* **1918**, *42*, 548.
(7) Richter, H.; Howard, J. B. *Prog. Energy Combust. Sci.* **2000**, *26*, 565 and references within.
(8) Frenklach, M. *Phys. Chem. Chem. Phys.* **2002**, *4*, 2028.
(9) Schuetzle, D.; Siegl, W. O.; Jensen, T. E.; Dearth, M.; Kaiser, E. W.; Gorse, R.; Kulik, E. *Environ. Health Perspect.* **1994**, *102(S4)*, 3.
(10) Chughtai, A. R.; Kim, J. M.; Smith, D. M. J. *Atmos. Chem.* **2003**, 45, 231.
(11) Asaba, T.; Fujii, N. *Symp. (Int.) Combust., [Proc.] 14th* **1971**, 155.
(12) Sloane, T. M. *J. Chem. Phys.* **1977**, *67*, 2267.
(13) Sibener, S. J.; Buss, R. J.; Casavecchia, P.; Hirooka, T.; Lee, Y. T. *J. Chem. Phys.* **1980**, *72*, 4341.
(14) Bittner, J. D.; Howard, J. B. *Symp. (Int.) Combust., [Proc.] 18th* **1981**, 1105.

10.1021/ja050173u CCC: $30.25

computational heats of reaction and rate constants for formation and destruction of the various intermediates observed in the oxidation mechanism. The model could be used to predict the concentrations of various intermediates as a function of time, and these results were then compared with the data available from experiments.[15,16] While several profiles were found to match well with experiment, such as the loss of benzene and the formation of CO, the concentration of phenoxy radical (C_6H_5O) was overestimated by a factor of about 100. Two possible explanations for this discrepancy were considered: either the rate constants for the formation or destruction of phenoxy radical were inaccurate, or a key mechanistic step was missing.[16]

The experimental rate constants for the formation of phenoxy radical have been supported by calculations. Hodgson and coworkers[17] have used CBS-QB3 and B3LYP electronic-structure models in combination with RRKM theory to determine rate constants for elementary channels of the reaction of C_6H_6 with $O(^3P)$. The standard mechanistic scheme continued to show an overestimation of the phenoxy radical concentration. This discrepancy may be due to intersystem crossing and conical intersections between the triplet and singlet potential energy surfaces. Since fairly high-level methods were used to compute the rate constants for the formation of phenoxy radical, it appeared unlikely that gross errors in their magnitudes could explain the discrepancy. Others have performed calculations on the decomposition pathways of the phenoxy radical, but again without resolution of the discrepancy.[18,19]

The low-temperature oxidation of benzene has been investigated because of its relevance to atmospheric chemistry.[20,21] Yu and Lin have studied the reaction of phenyl radical with O_2 at temperatures up to 473 K using cavity ring-down (CRD) spectroscopy. They observed only the formation of the $C_6H_5O_2$ adduct, phenylperoxy radical (**1**).[22] At higher temperatures, experiments by Venkat et al. indicated the presence of phenoxy radical (**6**).[23] Density functional theory (DFT) calculations using the B3LYP method show that the reaction of **1** going to **6** and $O(^3P)$ is relatively high in free energy at low temperatures. However, the free energy difference decreases with increasing temperature. In fact, the free energy difference becomes negative near 1200 K, which is in the range of combustion temperatures.[24,25]

We have proposed a new additional decomposition pathway for phenylperoxy radical, initially by use of PM3/UHF calculations (Scheme 1).[26] The pathway begins with a rearrangement to a spirodioxiranyl radical (**2**) followed by ring opening to the seven-membered ring, 2-oxepinoxy radical (**3**). The calculations were later refined at the B3LYP/6-311+G(d,p)//B3LYP/6-31G-(d) level.[24,25] The calculations found the free energy barrier for the rate-determining step in pathway A to be 42 kcal/mol from **1** to **2**, at 298 K. The free energy barrier for the rate-determining step in pathway B was shown to be 51 kcal/mol from **1** to **6**, at 298 K. The calculations also found **3** to reside in a deep local minimum with a free energy 80 kcal/mol below that of phenyl radical and O_2 (at 298 K and 1 atm). Pathway A is thermodynamically and kinetically more accessible than pathway B when $T < 432$ K.[24,27] Above 432 K, the decomposition of phenylperoxy radical to phenoxy radical and $O(^3P)$ is thermodynamically favored. The crossover temperature between the A and B channels could be higher if the decomposition of phenylperoxy radical faces a barrier, but that is still an open question. In any event, the calculations have provided evidence for an alternative pathway linking **1** to cyclopentadienyl radical, a known combustion product,[25,26] and might provide an explanation for the experimental observations outlined above.

Scheme 1. Two Proposed Mechanisms

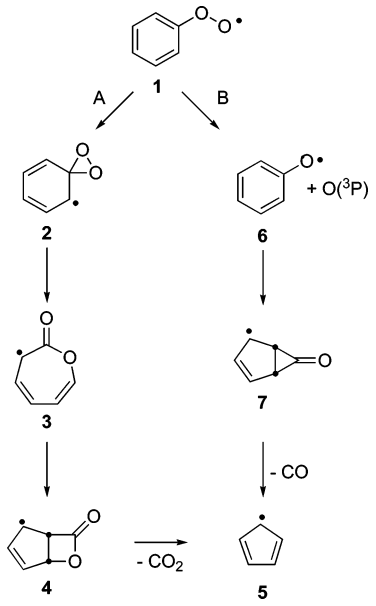

While theoretical evidence exists for the intermediacy of **3**, this premise is experimentally unsupported. We have consequently undertaken the generation of **3** and determination of its thermodynamic and kinetic properties. The present work is a contribution to the experimental determination of the heat of formation of **3**.

A method that can be used to experimentally determine heats of formation of radicals involves three separate experiments that make use of negative-ion thermodynamic cycles.[28] The three experiments find the gas-phase acidity (ΔH_{acid}) of an appropriate precursor (see below), the electron affinity (EA) of the radical, and the heat of formation of the precursor (ΔH_f). The first two of these steps are illustrated for the present example in eqs 4 and 5. A Hess's Law summation of these equations and that for electron capture by a proton leads to eq 7, showing that one can determine the homolytic bond-dissociation enthalpy (BDE) for H atom loss from the precursor. This quantity, in combina-

(15) Bittker, D. A. *Prog. Energy Combust. Sci.* **1991**, *79*, 49.
(16) Zhang, H.-Y.; McKinnon, J. T. *Combust. Sci. Technol.* **1995**, *107*, 261.
(17) Hodgson, D.; Zhang, H.-Y.; Nimlos, M. R.; McKinnon, J. T. *J. Phys. Chem. A* **2001**, *105*, 4316.
(18) Liu, R.; Morokuma, K.; Mebel, A. M.; Lin, M. C. *J. Phys. Chem.* **1996**, *100*, 9314.
(19) Olivella, S.; Sole, A.; Garcia-Raso, A. *J. Phys. Chem.* **1995**, *99*, 10549.
(20) Yamada, E.; Hosokawa, Y.; Furuya, Y.; Matsushita, K.; Fuse, Y. *Analytical Sciences* **2004**, *20*, 107.
(21) Schuetzle, D.; Siegl, W. O.; Jensen, T. E.; Dearth, M. A.; Kaiser, E. W.; Gorse, R.; Kreucher. W.; Kulik, E. *Environ. Health Persp.* **1994**, *102(S4)*, 3.
(22) Yu, T.; Lin, M. C. *J. Am. Chem. Soc.* **1994**, *116*, 9571.
(23) Venkat, C.; Brezinsky, K.; Glassman, I. *Symp. (Int.) Combust., [Proc.] 19th* **1982**, *143*.
(24) Barckholtz, C.; Fadden, M. J.; Hadad, C. M. *J. Phys. Chem. A* **1999**, *103*, 8108.
(25) Fadden, M. J.; Barckholtz, C.; Hadad, C. M. *J. Phys. Chem. A* **2000**, *104*, 3004.
(26) Carpenter, B. K. *J. Am. Chem. Soc.* **1993**, *113*, 9806.
(27) Barckholtz, C.; Barckholtz, T. A.; Hadad, C. M. *J. Phys. Chem. A* **2001**, *105*, 140.
(28) Berkowitz, J.; Ellison, G. B.; Gutman, D. *J. Phys. Chem.* **1994**, *98*, 2744.

tion with a calorimetric determination of the heat of formation of the precursor, leads finally to the desired heat of formation for the radical.

$$C_6H_6O_2 \rightarrow C_6H_5O_2^- + H^+ \qquad \Delta H_{acid} \tag{4}$$

$$C_6H_5O_2^- \rightarrow C_6H_5O_2 + e^- \qquad EA\ (C_6H_5O_2) \tag{5}$$

$$H^+ + e^- \rightarrow H \qquad -IP\ (H) \tag{6}$$

$$C_6H_6O_2 \rightarrow C_6H_5O_2 + H \qquad BDE = \Delta H_{acid} + EA - IP \tag{7}$$

$$\Delta H_f\,(C_6H_5O_2) = BDE + \Delta H_f\,(H) - \Delta H_f\,(C_6H_6O_2) \tag{8}$$

As a first step in the determination of the ΔH_f of **3**, we report here the synthesis of 2(3H)-oxepinone (**12b**) as well as the results of a bracketing study to determine its gas-phase acidity using the flowing afterglow technique.

II. Experimental Section

A. Chemical Synthesis of 2-(3H)-Oxepinone (12b). General Methods. Tetrahydrofuran (THF) was purified by distillation from sodium benzophenone ketyl. CCl_4 was dried over 5 Å molecular sieves. CH_2Cl_2 was purified by distillation over CaH_2. All commercially available reagents were used as supplied from Aldrich or Acros Chemicals. ^{1}H NMR spectra were recorded on a Varian INOVA 400 spectrometer at 399.78 MHz. ^{13}C NMR spectra were recorded on a Varian Mercury 300 spectrometer at 75.38 MHz. All NMR spectra were taken in $CDCl_3$ with chemical shifts given in parts per million (δ) with respect to the residual solvent peak.[29] Coupling constants are given in hertz. Two-dimensional (2D) NMR spectra were recorded on a Varian INOVA 600. COSY, HSQC, and HMBC 2D NMR spectra were acquired using the standard Varian gradient pulse sequences. Infrared (IR) spectra were acquired on KBr plates with a Nicolet Impact 410 FT-IR spectrometer. Gas chromatography (GC) was performed with a Hewlett-Packard 6890 GC equipped with a flame ionization detector (FID). Preparative GC was performed with a Varian Aerograph 202C equipped with a thermal conductivity detector (TCD) at an oven temperature of 160 °C and a detector temperature of 200 °C. For the preparative GC, a glass column (4.75−5 m × 7−8m × 4−5 mm) was packed with 25% $Me_3SiO-(SiO)_n-SiMe_2CH_2CH_2CF_3$ on 60/80 mesh Chromosorb W-HP. Low resolution mass spectrometry (LRMS) was performed with a Hewlett-Packard 5890 GC equipped with a Hewlett-Packard 5970 mass selective detector and given in units mass per charge (*m*/*z*). Accurate mass molecular formula confirmation of **12b** was obtained via high-resolution MS and was performed at the Ohio State University Chemistry MS facility using 70 eV electron impact ionization with a Kratos MS-25 sector instrument. Thin-layer chromatography (TLC) was performed on glass plates coated with 0.25 mm 60 F_{254} silica gel and visualized with UV light and I_2 stain. Silica gel 60 (0.040−0.063 mm particle size) was used for all flash column chromatography. Air- and moisture-sensitive reactions were conducted in oven-dried glassware under an atmosphere of Ar or N_2.

3-Bromo-2-oxepanone (9). To a cooled solution (ice/NaCl bath) of trimethyl[(4,5,6,7-tetrahydro-2-oxepinyl)oxy]silane[30] (**8**) (45 g, 0.24 mol) and Et_3N (18 mL, 0.13 mol) in CH_2Cl_2 (600 mL) was added Br_2 (12 mL, 0.24 mol) dropwise over 5 min with evolution of HBr. After stirring for 20 min, the solution was brought to room temperature (rt). The solution was then washed with 10% (aq) NH_4Cl (2 × 300 mL), dried over $MgSO_4$, filtered, and concentrated in vacuo. The crude product was purified by flash chromatography on silica (Et_2O/pentane, 3:2) to yield **9** (36 g, 78%) as a yellow oil: IR (neat, cm^{-1}) 2930, 2873, 1752, 1711, 1470, 1143; ^{1}H NMR (400 MHz, $CDCl_3$) δ 4.87−4.83 (m, 1H), 4.77−4.69 (m, 1H), 4.33−4.22 (m, 1H), 2.17−1.76 (m, 6H); ^{13}C NMR (75 MHz, $CDCl_3$) δ 169.91, 69.88, 48.38, 31.95, 29.27, 25.42; MS (*m*/*z*) 194, 192, 108, 106, 69, 42, 27.

6,7-Dihydro-2(5H)-oxepinone (10a) and 6,7-Dihydro-2(3H)-oxepinone (10b). To a solution of **9** (36 g, 0.19 mol) in THF (400 mL) was added 1,8-diazabicyclo[5.4.0]undec-7-ene (DBU) (32 mL, 0.21 mol) dropwise over 5 min. The solution was then heated to 70 °C for 3 h. The solution was cooled to room temperature, filtered, and concentrated in vacuo. The crude residue was purified by flash chromatography on silica (Et_2O/pentane, 5:1) to yield **10b:10a** (2.5:1, 16 g, 75%) as a slightly yellow oil. Each species was isolated, and respective ^{1}H NMR spectra agreed with literature values.[31]

5-Bromo-6,7-dihydro-2(5H)-oxepinone (11). A solution of **10b:10a** (2.5:1, 16 g, 0.14 mol), *N*-bromosuccinimide (26 g, 0.14 mmol), and benzoyl peroxide (1.7 g, 10 mmol) in CCl_4 (250 mL) was heated at reflux for 6 h. The solution was cooled to room temperature, filtered, and concentrated in vacuo. The crude product was purified by flash chromatography on silica (Et_2O/pentane, 1:1) to yield **11** (16 g, 60%) as an oil. The ^{1}H NMR spectrum of the product agreed with that reported by Busque et al.[32]

2(3H)-Oxepinone (12b). To a solution of **11** (16 g, 84 mmol) in THF (400 mL) was added DBU (13 mL, 85 mmol). The solution was heated to 40 °C for 2 h. The solution was cooled to room temperature, filtered, and concentrated in vacuo. The crude product was purified by flash chromatography (Et_2O/pentane, 3:1) to yield 2(7H)-oxepinone (**12a**) (6.1 g, 65%) as a yellow oil: IR (neat, cm^{-1}) 3048, 2919, 1768, 1706, 1421, 1375, 1262, 1174; ^{1}H NMR (400 MHz, $CDCl_3$) δ 6.74 (ddd, J = 11.8, 4.0, 2.0, 1H-4), 6.55−6.53 (m, 1H-5, 1H-6), 6.46 (d, J = 11.9, 1H-3), 4.56 (d, J = 5.7, 2H-7); ^{13}C NMR (75 MHz, $CDCl_3$) δ 168.85 (C-2), 137.41 (C-4), 133.00−132.96 (C-5, C-6), 125.99 (C-3), 62.17 (C-7); MS (*m*/*z*) 110, 82, 53, 39.

Further purification by either preparative GC or vacuum distillation (80−90 °C, 0.1 Torr) led to **12b** (2.4 g, 26% from **11**) as a yellow oil: IR (neat, cm^{-1}) 3047, 1758, 1602, 1260, 1111, 1079; ^{1}H NMR (400 MHz, $CDCl_3$) δ 6.54 (d, J = 6.8, 1H-7), 6.20 (dd, J = 9.2, 5.2, 1H-5), 5.85 (dd, J = 7.0, 5.3, 1H-6), 5.77 (dt, J = 9.1, 6.8, 1H-4), 3.04 (d, J = 6.8, 2H-3); ^{13}C NMR (75 MHz, $CDCl_3$) δ 166.06 (C-2), 140.92 (C-7), 127.20 (C-5), 122.55 (C-4), 112.66 (C-6), 36.39 (C-3); MS (*m*/*z*) 110, 82, 53, 39; HRMS exact mass calcd for $C_6H_6O_2$ *m*/*z* 110.0362, found *m*/*z* 110.0374. (See Results and Discussion and Supporting Information for 2D NMR results.)

B. Experimental Determination of the Gas-Phase Acidity of 2(3H)-Oxepinone. The flowing afterglow technique has been used to examine the gas-phase acidity of a purified sample of **12b** by means of a bracketing study. Our flowing afterglow apparatus has been described previously.[33,34] A description of the conditions used in these particular experiments follows.

To perform the bracketing study, anions were generated by way of electron ionization (EI). These ions then traveled the length of a flow tube in the presence of a buffer gas of helium. The flow rate was maintained to give a flow tube pressure of ~0.4 Torr. The temperature of the helium buffer gas was 30 °C. Hydroxide anion was produced by dissociative electron capture of N_2O, resulting in O^-, and then subsequent H-atom abstraction from methane gas (CH_4), thereby producing HO^-. All other bases (X^-) were then generated by the reaction of HO^- with the appropriate neutral precursor (X−H) in the ion source. Anions were produced by proton transfer from MeOH, EtOH, CH_3CHO, pyrrole, CH_3CO_2H, $HC(O)NH_2$, H_2S, *t*-BuSH, and $CH_3CH_2CH_2SH$. The sample of the neutral **12b** was introduced via a

(29) Gottlieb, H. E.; Kotlyar, V.; Nudelman, A. *J. Org. Chem.* **1997**, *62*, 7512.
(30) Christoffers, J.; Oertling, H.; Fischer, P.; Frey, W. *Tetrahedron* **2003**, *59*, 3769.
(31) Detrembleur, C.; Mazza, M.; Lou, X.; Halleux, O.; Lecomte, P.; Mecerreyes, D.; Hedrick, J. L.; Jérôme, R. *Macromolecules* **2000**, *33*, 7751.
(32) Busque, F.; Cid, P.; de March, P.; Figueredo, M.; Font, J. *Heterocycles* **1995**, *40*, 387.
(33) Frink, B. T.; Hadad, C. M. *J. Chem. Soc., Perkin Trans. 2* **1999**, 2397.
(34) Cohen, M. H.; Barckholtz, C.; Frink, B. T.; Bond, J. J.; Geise, C. M.; Hoff, J.; Herlinger, J.; Hickey, T.; Hadad, C. M. *J. Phys. Chem. A* **2000**, *104*, 11318.

Scheme 2. Synthesis of **12b**

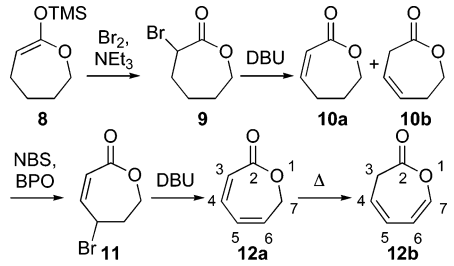

heated bulb (ca. 50 °C) through an inlet located approximately 30 cm downstream from the ion source. The resulting spectra were monitored in the range of *m*/*z* 10−180 for the disappearance of the initial anion and appearance of the M − 1 (*m*/*z* 109) species of **12b**.

Reactions were also performed in the reverse direction for verification purposes by production of MeO^- in the ion source as described above. Neutral **12b** was introduced via the same method and inlet described above. Neutral reagents, such as acetic acid, hydrogen sulfide, *tert*-butylmercaptan, nitromethane, and 1,1,1,3,3,3-hexafluoro-2-propanol were introduced via fixed inlets in the ∼0.5 m reaction zone of the flow tube. The *m*/*z* spectra were monitored from proton transfer by examination of the loss of signal for the M − 1 (*m*/*z* 109) species of **12b** and concomitant appearance of the M − 1 species for the neutral reagent. Because sufficient vapor pressure of **12b** could not be generated, residual MeO^- was left in the ion stream, and therefore the reaction could only be monitored by examining the change in ion signal for *m*/*z* 109 before and after the neutral reagent was introduced.

C. Computational Methods. Stationary points were calculated using Becke's three parameter hybrid exchange functional[35,36] with the Lee−Yang−Parr correlation functional (B3LYP) using the 6-31+G(d) basis set.[37−39] The accuracy of the DFT method was also checked for some of the neutral species by carrying out CBS-QB3 calculations.[39b] Basis-set truncation effects were explored by carrying out some of the calculations with the aug-cc-pVTZ basis set.[40] Each stationary point was confirmed to be either a minimum or transition state on the basis of a harmonic vibrational frequency calculation having zero or one imaginary vibrational frequency, respectively. Transition states were verified to connect to the appropriate intermediates by displacing the transition state structure along the vector for the normal coordinate by ±10%, followed by careful optimization (opt = calcfc). An intrinsic reaction coordinate (IRC) was performed to verify the connectivity in TS(**15a**−**27**). Zero-point energy (ZPE) corrections were obtained and scaled by a factor of 0.9806 for the B3LYP/6-31+G(d) calculations.[41] All energies cited in the text are $\Delta_{rxn}G_{298}$ with respect to a 1 atm and 298 K standard state, unless otherwise stated. All calculations were performed with the GAUSSIAN 98[42] or GAUSSIAN 03[43] suites of programs.

III. Results and Discussion

A. Synthesis of 12b. The synthesis of **12b** is summarized in Scheme 2. The first step was based on a similar synthesis involving bromination of the trimethylsilyl-trapped enolate of δ-valerolactone.[44] The reaction of **8**[30] with Br_2 led to **9** in 78% isolated yield. Although **9** has been previously reported,[45] spectral data were not published, and so they are given in the Experimental Section.

Scheme 3. Reaction of **13** with DBU

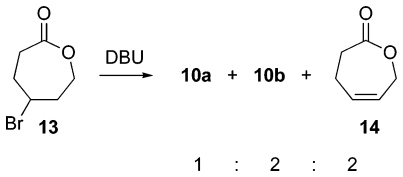

In the next step, the strategy was to eliminate HBr from **9** to give **10a**; however, elimination with DBU led to **10b** as the major product with **10a** as only a minor product. The product ratio of **10b:10a** was 2.5:1 with a total isolated yield of 75%. The elimination was attempted under kinetic control with stronger bases, such as lithium ethoxide and potassium *tert*-butoxide, but all attempts led to degradation of the starting material without production of **10a** or **10b**. The stability of **10b** with respect to that of **10a** was examined using B3LYP/6-31+G-(d) calculations, which showed that **10b** is favored by 1.1 kcal/mol. In a similar reaction, Detrembleur and co-workers[31] found that the elimination of 5-bromo-2-oxepanone (**13**) with DBU led to a mixture of **10a**, **10b**, and 4,7-dihydro-2(3H)-oxepinone (**14**) in an isolated ratio of about 1:2:2, respectively (Scheme 3). Our results along with those of Detrembleur et al. suggest that **10b** is in equilibrium with and is more stable than **10a**.

In the next step, the purified mixture of **10a** and **10b** was treated with an equivalent of *N*-bromosuccinimide and a catalytic amount of benzoyl peroxide in CCl_4 at reflux to give **11** as the major product in 60% yield after purification. In addition to **11**, GC and GC/MS data showed the presence of other products, all in such low yield that their isolation and identification were not attempted. However, a small amount (ca. 10% by GC) of **12a** was found along with purified **11**. In the final step, the purified products from the previous step were treated with DBU at an elevated temperature to yield **12a**. B3LYP/6-31+G(d) calculations determined **12b** to be lower in free energy than **12a** by 3.0 kcal/mol. CBS-QB3 calculations gave a similar result (3.7 kcal mol in favor of **12b**). Isomerization of **12a** to **12b** did not take place under the reaction conditions; however, it did occur under final purification conditions of either preparative GC or vacuum distillation, both of which afforded **12b** as the only distinguishable isomer in the ^1H NMR spectrum. This finding suggested that there exists a substantial barrier to the isomerization, and that the equilibrium favors **12b** by at least 3.6 kcal/mol.[46] The finding that **12b** is more stable than **12a** is consistent with the results of Hoshi et al. on substituted oxepinones. They have reported the synthesis and subsequent isomerizations of 3-isopropyl-2(7H)-oxepinone, 7-phenyl-2(7H)-oxepinone, and 3-methyl-7-phenyl-2(7H)-oxepinone to their respective 2(3H) isomers at room temperature.[47]

(35) Parr, R. G.; Yang, W. *Density-Functional Theory of Atoms and Molecules*; Oxford University Press: New York, 1989.
(36) Labanowski, J. W.; Andzelm, J. *Density Functional Theory in Chemistry*; Springer: New York, 1991.
(37) Becke, A. D. *J. Chem. Phys.* **1993**, *98*, 5648.
(38) Lee, C.; Yang, W.; Parr, R. G. *Phys. Rev. B* **1988**, *37*, 785.
(39) (a) Hehre, W. J.; Radom, L.; Schleyer, P. v. R.; Pople, J. A. *Ab Initio Molecular Orbital Theory*; John Wiley & Sons: New York, 1986. (b) Montgomery, J. A., Jr.; Frisch, M. J.; Ochterski, J. W.; Petersson, G. A. *J. Chem. Phys.* **1999**, *110*, 2822.
(40) Dunning, T. H., Jr. *J. Chem. Phys.* **1989**, *90*, 1007. Woon, D. E.; Dunning, T. H., Jr. *J. Chem. Phys.* **1994**, *100*, 2975.
(41) Scott, A. P.; Radom, L. *J. Phys. Chem.* **1996**, *100*, 16502.
(42) Frisch, M. J. et al. *Gaussian 98*, Revision A.9; Gaussian, Inc.: Pittsburgh, PA, 1998.
(43) Frisch, M. J. et al. *Gaussian 03*, Revision B.05; Gaussian, Inc.: Pittsburgh, PA, 2003.
(44) Wolff, J. J.; Frenking, G.; Harms, K. *Chem. Ber.* **1991**, *124*, 551.
(45) Silks, L. A., III; Odom, J. D.; Dunlap, R. B. *Synth. Commun.* **1991**, *21*, 1105.
(46) It is assumed that 1% or more of the minor isomer could be detected using ^1H NMR spectroscopy. Since we do not detect the minor isomer, the equilibrium constant (*K*) is assumed to be equal to or greater than 100. The isomerization is completed ca. 400 K, using $\Delta G = -RT \ln K$; $\Delta G = -3.6$ kcal/mol for the conversion of **12a** to**12b**.
(47) Hoshi, N.; Sato, K.; Uda, H.; Hagiwara, H. *J. Chem. Res.* **1984**, *12*, 3501.

Table 1. ^{1}H NMR, ^{13}C NMR, and gHMBC Results for **12a**

position	δ ^{13}C (ppm)[a]	δ ^{1}H (ppm)[b]	HMBC correlations
2	168.85	–	–
3	125.99	6.46	C-2, C-4, C-5, C-6, C-7
4	137.41	6.74	C-2, C-3, C-5, C-6, C-7
5/6	133.0−132.96	6.55−6.53	C-3, C-4, C-7
7	62.17	4.56	C-2, C-5, C-6

[a] Assignments are based on the ^{1}H NMR spectrum and confirmation with a COSY experiment. [b] Assignments are based on an HSQC experiment.

Table 2. ^{1}H NMR, ^{13}C NMR, and gHMBC Results for **12b**

position	δ ^{13}C (ppm)[a]	δ ^{1}H (ppm)[b]	HMBC correlations
2	166.06	–	–
3	36.39	3.04	C-2, C-4, C-5, C-6, C-7
4	122.55	5.77	C-2, C-3, C-5, C-6, C-7
5	127.20	6.20	C-2, C-3, C-5, C-6, C-7
6	112.66	5.85	C-4, C-7
7	140.92	6.54	C-2, C-5, C-6, C-7

[a] Assignments are based on the ^{1}H NMR spectrum and confirmation with a COSY experiment. [b] Assignments are based on an HSQC experiment.

The identities of **12a** and **12b** were determined by using conventional 1D ^{1}H and ^{13}C NMR spectroscopy, as well as a variety of 2D NMR techniques. The ^{1}H NMR chemical shifts for the methylene groups in **12a** and **12b** were found to be 4.56 and 3.02 ppm, respectively. This finding is consistent with the former isomer being the one with the methylene group singly bonded to oxygen.[48] Chemical shifts in the ^{1}H and ^{13}C NMR spectra were assigned by COSY and HSQC experiments (see Tables 1 and 2). Carbon−carbon connectivity was deduced using long-range ^{1}H−^{13}C heteronuclear multiple bond coherence (HMBC).[49] HMBC spectra of **12a** and **12b** provided unambiguous evidence supporting the assigned structures (see Tables 1 and 2). In the HMBC spectra, the four-bond C-2, H-6 correlation of **12b** was not observed, whereas the three-bond C-2, H-4 correlation of **12a** was observed. Additional information in the HMBC spectra was that the four-bond C-2, H-6 correlation of **12a** was not observed, while the three-bond C-2, H-4 correlation of **12b** was observed. Hence, HMBC, COSY, and HSQC 2D NMR experiments allowed the structural assignments of isomers **12a** and **12b**.

B. Gas-Phase Acidity Bracketing Study. The results of the bracketing study for the deprotonation of **12b** are provided in Table 3. In these reactions, the appropriate X^- was generated and allowed to react with neutral **12b**, and the formation of the anion of **12b** (*m*/*z* 109) was monitored. Also included in the table are the previously reported gas-phase acidities for the known species used in this study.[50] As can be observed from the table, **12b** was successfully deprotonated by HO^-, CH_3O^-, EtO^-, $^-CH_2CHO$, $HC(O)NH^-$, pyrrole anion, $^-CH_2NO_2$, $CH_3CH_2CH_2S^-$, and *t*-BuS^-.

In all of the reactions studied herein, proton transfer was the dominant reaction pathway. In the cases of the reaction of the alkoxides (methoxide and ethoxide) as well as hydroxide ion, another pathway was also observed. In each of these cases, a signal at *m*/*z* 65 was observed. This signal is due to loss of CO_2 from the anion of **12b** (see Schemes 6 and 7 for proposed structures). In all of the other anionic reactions, only proton transfer was observed with **12b**.

Table 3. Reactions of Anions Produced from Known Acids with **12b**

acid (X–H)	gas-phase acidity ($\Delta_{acid}H_{298}$)[a]	gas-phase acidity ($\Delta_{acid}G_{298}$)[a]	proton transfer?
water	390.3	383.70 ± 0.20	yes
methanol	382.20 ± 0.7	375.10 ± 0.6	yes
ethanol	378.3 ± 1.0	371.7 ± 1.1	yes
acetaldehyde	365.8 ± 2.2	359.0 ± 2.0	yes
formamide	359.8 ± 2.1	352.8 ± 2.0	yes
pyrrole	358.6 ± 2.2	350.9 ± 2.0	yes
propanethiol	354.2 ± 2.2	347.9 ± 2.0	yes
tert-butylthiol	352.5 ± 2.2	346.2 ± 2.0	yes
hydrogen sulfide	351.3 ± 0.10	344.9 ± 0.10	no
acetic acid	348.1 ± 2.2	341.1 ± 2.0	no

[a] In kcal/mol, from http://webbook.nist.gov (see ref 50).

However, **12b** was not deprotonated by HS^- or $CH_3CO_2^-$. It was not possible to generate sufficient amounts of the anion of 1,1,1,3,3,3-hexafluoro-2-propanol due to the tendency of the anion to form clusters with its precursor. There was also difficulty in generating the $O_2NCH_2^-$ anion cleanly in the ion source without contamination by undesired NO_2^-. (For annotated spectra of the above reactions, see the Supporting Information.) From the data presented above, it is apparent that the gas-phase acidity of **12b** lies above that of H_2S and below that of *t*-BuSH. This observation suggests that the gas-phase acidity ($\Delta_{acid}H_{298}$) for **12b** is in the range of 351.3−352.5 kcal/mol.

To confirm the gas-phase acidity determined above, the reverse reactions were also performed. The anion of **12b** was produced through a proton-transfer reaction with MeO^-. The *m*/*z* 109 anion was then reacted with a series of acids of known gas-phase acidities. By examining the change in the M − 1 signal for **12b** (*m*/*z* 109), it was possible to determine whether the anion successfully accomplished a proton-transfer reaction with the known acid. Once again, only proton-transfer reactions were observed. The results for this portion of the bracketing study are provided in Table 4. (Annotated spectra for each of the reactions can be found in the Supporting Information.) These data confirm that the gas-phase acidity of **12b** does, in fact, lie between that of H_2S and *t*-BuSH. In separate experiments, we confirmed that the anions from propanethiol and *tert*-butylthiol could accomplish a proton-transfer reaction with H_2S. We also confirmed that the reverse reactions (HS^- with either PrSH or *t*-BuSH) did not proceed. Therefore, there appears to be no kinetic limitations to using these thiols for rapid proton-transfer reactions in a bracketing study.

(48) Silverstein, R. M.; Webster, F. X. *Spectrometric Identification of Organic Molecules*, 6th ed.; John Wiley and Sons: New York, 1998; Chapter 4.

(49) A difference in C−C connectivity between **12a** and **12b** is the location of the methylene groups' carbon with respect to the carbonyls' carbon. To explore this difference, a rather time-expensive incredible natural abundance double quantum transfer experiment (INADEQUATE) could be performed. Although, a much simpler and faster experiment that we conducted was a proton-detected, long-range ^{1}H−^{13}C heteronuclear multiple bond coherence (HMBC) experiment. While INADEQUATE experiments show adjacent ^{13}C−^{13}C couplings, HMBC experiments typically show both two- and three-bond ^{1}H−^{13}C couplings ($^2J_{CH}$ and $^3J_{CH}$), while occasionally four-bond ^{1}H−^{13}C couplings ($^4J_{CH}$) are observed.

(50) http://webbook.nist.gov. (a) Water: Schulz, P. A.; Mead, R. D.; Jones, P. L.; Lineberger, W. C. *J. Chem. Phys.* **1982**, *77*, 1153. (b) Methanol: DeTuri, V. F.; Ervin, K. M. *J. Phys. Chem. A* **1999**, *103*, 6911. (c) Ethanol: Ramond, T. M.; Davico, G. E.; Schwartz, R. L.; Lineberger, W. C. *J. Chem. Phys.* **2000**, *112*, 1158. (d) Acetaldehyde, pyrrole, propanethiol, *tert*-butylthiol, nitromethane: Bartmess, J. E.; Scott, J. A.; McIver, R. T., Jr. *J. Am. Chem. Soc.* **1979**, *101*, 6047. (e) Formamide: Taft, R. W. *Prog. Phys. Org. Chem.* **1987**, *16*, 1. (f) Hydrogen sulfide: Breyer, F.; Frey, P.; Hotop, H. *Z. Phys. A* **1981**, *300*, 7. (g) Acetic acid: Taft, R. W.; Topsom, R. D. *Prog. Phys. Org. Chem.* **1987**, *16*, 1. (h) 1,1,1,3,3,3-Hexafluro-2-propanol: Taft, R. W.; Koppel, I. J.; Topsom, R. D.; Anvia, F. *J. Am. Chem. Soc.* **1990**, *112*, 2047.

Table 4. Reactions of the Anion of **12b** with a Variety of Neutral Acids

acid (X–H)	gas-phase acidity ($\Delta_{acid}H_{298}$)[a]	gas-phase acidity ($\Delta_{acid}G_{298}$)[a]	proton transfer?
nitromethane	356.4 ± 2.2	349.7 ± 2.0	no
tert-butylthiol	352.5 ± 2.2	346.2 ± 2.0	no
hydrogen sulfide	351.3 ± 0.10	344.9 ± 0.10	yes
acetic acid	348.1 ± 2.2	341.1 ± 2.0	yes
1,1,1,3,3,3-hexafluoro-2-propanol	345.0 ± 2.1	338.4 ± 2.0	yes

[a] In kcal/mol, from http://webbook.nist.gov (see ref 50).

Scheme 4. Gas-Phase Acidities ($\Delta_{Acid}H_{298}$) of **12b** for Deprotonation at C-3 (**15a**), C-6 (**15b**), and C-7 (**15c**), Calculated at the B3LYP/6-31+G(d) Level (normal text) and at the B3LYP/aug-cc-pVTZ Level (bold text) and Reported in kcal/mol

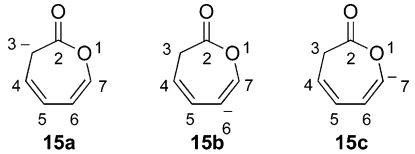

15a 348.9 **349.2** | **15b** 377.4 **376.1** | **15c** 379.2 **381.2**

On the basis of the data collected in this bracketing study, the gas-phase acidity of **12b** has been determined and confirmed in both the forward and reverse directions. Unfortunately due to the limited volatility of **12b**, rate coefficients could not be performed for an equilibrium acidity determination. From the bracketing study, the gas-phase acidity lies between those of hydrogen sulfide ($\Delta_{acid}H_{298} = 351.3 \pm 0.10$ kcal/mol) and *tert*-butylthiol ($\Delta_{acid}H_{298} = 352.5 \pm 2.2$ kcal/mol). These data lead us to assign the gas-phase acidity values for **12b** as $\Delta_{acid}H_{298} = 352 \pm 2$ kcal/mol and $\Delta_{acid}G_{298} = 346 \pm 2$ kcal/mol.

C. Discussion

The interpretation of the flowing afterglow experimental results is predicated on the assumptions that the anion generated was indeed **15a** and that it was stable once formed. These issues were explored computationally. The gas-phase acidity ($\Delta_{acid}H_{298}$) of heterolysis of the C-3, H-3 bond of **12b** was calculated at the B3LYP/aug-cc-pVTZ and was 349.2 kcal/mol (Scheme 4). For comparison, removal of the next most acidic proton in **12b** (heterolysis of the C-6, H-6 bond, leading to **15b**) led to a gas-phase acidity value of 376.1 kcal/mol at the same level of theory. We judge the large difference to be outside of the likely error in the calculations.[51] That conclusion and the similarity of the computed acidity for **15a** to the experimental acidity are together taken as support for the assignment of structure **15a** to the anion. The flowing afterglow results demonstrated that the anion proposed to be **15a** reacts with proton sources and that the gas-phase acidity of its conjugate acid agrees with that deduced for **12b** by deprotonation. This result implies that the anion is stable, unless it rearranged to an isomer of coincidentally identical basicity.

To be more certain of the stability of **15a** once formed, potential rearrangement pathways were examined at the B3LYP/6-31+G(d) level (Scheme 5). Two ring-opening pathways were considered, including heterolysis of the O-1, C-2 and O-1, C-7 bonds. The products, **16** and **17**, are higher in free energy than **15a** by 6.8 and 7.4 kcal/mol, respectively. Also, the free energies

(51) Baker, J.; Muir, M.; Andzelm, J. *J. Chem. Phys.* **1995**, *102*, 2063.

Scheme 5. Plausible Rearrangement Pathways of **15a**; Intermediates Calculated Using B3LYP/6-31+G(d) with Energies Reported as $\Delta_{rxn}G_{298}$ with Respect to **15a** in kcal/mol.

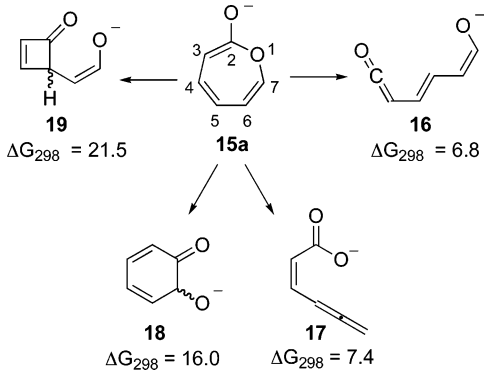

19 ΔG_{298} = 21.5 | **15a** | **16** ΔG_{298} = 6.8

18 ΔG_{298} = 16.0 | **17** ΔG_{298} = 7.4

for anions **18** and **19** were calculated, perhaps resulting from nucleophilic attack of either C-7 or C-5 on C-2, followed by ring opening. Both **18** and **19** are higher in energy than **15a** by 16.0 and 21.5 kcal/mol, respectively. The results of the calculations are that intermediates **16**−**19** are not predicted to be formed under the experimental conditions. However, there may be a viable rearrangement pathway, and it will be discussed below.

Of possible significance for future photodetachment studies was the finding of a nonplanar structure for **15a** at the B3LYP/6-31+G(d) and the B3LYP/aug-cc-pVTZ levels. The latter level found the planar structure (C_s symmetry) to be only 2.5 kcal/mol higher in enthalpy than the nonplanar structure, although it was a transition state for interconversion of the nonplanar enantiomers. The calculations thus suggest that the photoelectron spectrum of anion **15a** could exhibit a significant vibrational progression corresponding to the out-of-plane bending of the ring.

For a better understanding of the deprotonation pathway, part of the potential energy surface (PES) for the deprotonation of **12b** by methoxide anion was calculated (see Figure 1). Prior to deprotonation, **12b** and methoxide first form an ion−dipole complex (**20**) which is exergonically formed by 9.2 kcal/mol. The reaction then proceeds through a transition state where the C−H bond in **12b** is being broken by forming an O−H bond with methoxide anion. The energy of the transition state is 4.9 kcal/mol above the energy of **20** and 4.3 kcal/mol below the energy of **12b** and methoxide. The transition state leads to a product ion−dipole complex (**21**), 28.2 kcal/mol below the energy of **12b** and methoxide, where **15a** and methanol are in a complex that can dissociate. The final products **15a** and methanol are formed exergonically by 28.1 kcal/mol, with respect to **12b** and methoxide.

The flowing afterglow experiments demonstrated that **12b** reacts with strong bases to form an ionic product with *m*/*z* 65 (see above). A plausible mechanistic route leading to this product is an elimination reaction, where the base abstracts a proton from the C-6 position of **12b**. The proton abstraction can lead to formation of an alkyne with the carboxylate group serving as the leaving group. Decarboxylation of **25** can then occur to form **26**, which has the appropriate mass to fit the experimental observation (Scheme 6). B3LYP/6-31+G(d) calculations were used to explore the stationary points for this elimination pathway with methoxide as the base. The energies of the stationary points in Scheme 6 and in the following

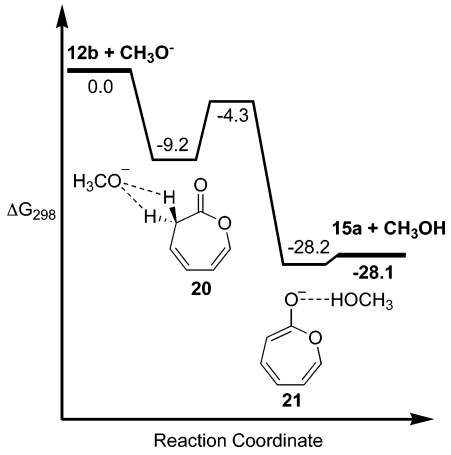

Figure 1. PES for deprotonation reaction of **12b** by methoxide anion calculated at the B3LYP/6-31+G(d) level with energies reported as $\Delta_{rxn}G_{298}$ in kcal/mol.

Scheme 6. Elimination Pathway of **12b**[a]

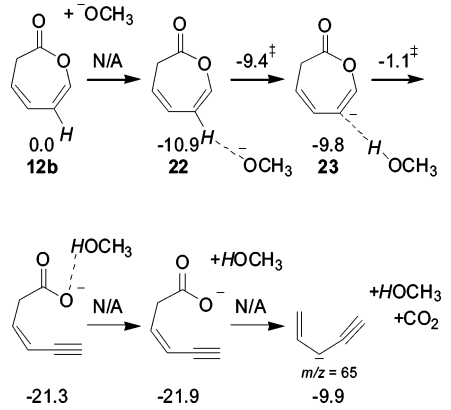

[a] Stationary points were calculated at the B3LYP/6-31+G(d) level of theory. All energies are reported as $\Delta_{rxn}G_{298}$ with respect to **12b** and methoxide. Transition-state energies are above the arrows, and minimum energies are given below the appropriate structures.

discussion are relative free energies with respect to **12b** and methoxide. The mechanism first involves exergonic (−10.9 kcal/mol) formation of a complex (**22**) between **12b** and methoxide. The first transition state (**TS 22**−**23**) involves the transfer of a proton from **12b** to methoxide and has a free energy of −9.4 kcal/mol. This transition state leads to a complex (**23**) between methanol and the carbanion at a free energy of −8.9 kcal/mol. The next step is the elimination reaction, leading to a complex (**24**) between methanol and the carboxyalkyne anion (**25**). The transition state leading to **24** has a free energy of −1.1 kcal/mol, and the free energy of **24** is −21.3. Methanol and **25** are not tightly bound, and the dissociated species have a free energy of −21.9 kcal/mol. The final step of the process is the decarboxylation. A transition state search was not successful, and an energy surface scan by increasing the bond length of the breaking C−C bond did not show a maximum (see Figure 2 in Supporting Information). Therefore, this decarboxylation step appears to proceed without a barrier leading to the anionic product **26** and methanol, which have a free energy of −9.9 kcal/mol. All of the stationary points within the elimination mechanism have energies less than that of **12b** and methanol.

Another experimental observation is that the product of *m*/*z* 65 is only formed in the reaction of **12b** with the most basic anions. This product is not observed, for instance, in the reaction

Scheme 7. Rearrangement Pathway of **15a**[a]

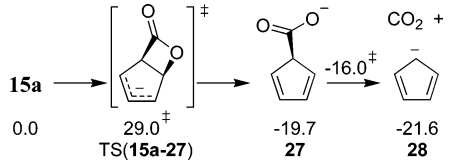

[a] Stationary points were calculated at the B3LYP/6-31+G(d) level of theory. All energies are reported as $\Delta_{rxn}G_{298}$ with respect to **15a**. Transition-state energies are shown with double-dagger symbol, and energies for local minima are given below the appropriate structures.

of **12b** with the anion of acetaldehyde ($\Delta_{acid}H_{298}$ = 365.8 kcal/mol). We chose to examine the potential energy surface for the elimination process with fluoride, which has a low basicity (see Scheme 8 in the Supporting Information). The mechanism found was similar to that with methoxide. However, the net free energy barrier for this reaction is 3.2 kcal/mol above the reactants.

A reviewer has suggested another route for the formation of the *m*/*z* 65 product observed in the gas-phase experiments. It consists of an electrocyclic ring closure of **15a**, followed by ring opening and decarboxylation (Scheme 7). B3LYP/6-31+G-(d) calculations revealed a transition state between **15a** and **27**, with a free energy barrier of 29.0 kcal/mol above the energy of **15a**. An intrinsic reaction coordinate (IRC) verified that TS (**15a**−**27**) connected **15a** and **27**, and showed that the bicyclic anion was not a local minimum at this level of theory. The free energy of **27** was calculated to be −19.7 kcal/mol below that of **15a**. Decarboxylation of **27** had a low barrier; the products were found to have a free energy of −21.6 kcal/mol with respect to **15a**. The experimental observation that the formation of the *m*/*z* 65 product was formed only with strong bases could be consistent with this mechanism, because weaker bases might not generate **15a** with enough internal energy to surmount the barrier to electrocyclization.

Comparison of the two pathways proposed for formation of the *m*/*z* 65 ion shows that the highest barriers for each process are similar in free energy. The barrier for the E2 pathway is 2.0 kcal/mol lower than that for the electrocyclic ring closure pathway. This difference is within the probable error of the calculations used.[51] Consequently, we offer no conclusion as to which *m*/*z* 65 is more likely. It is quite possible that both occur.

IV. Conclusion

The synthesis of the previously unknown 2(7H)-oxepinone (**12a**) and 2(3H)-oxepinone (**12b**) has been achieved by elimination of HBr from the previously reported 5-bromo-6,7-dihydro-2(5H)-oxepinone (**12**). We have determined the gas-phase acidity ($\Delta_{acid}H_{298}$) of **12b** through a bracketing study using a flowing afterglow apparatus with quadrupole mass spectrometric detection. In the reactions of **12b** with a series of bases in the gas phase, a proton-transfer reaction was observed when **12b** was reacted with *t*-BuS^-, whereas none was observed when **12b** was reacted with HS^-. Therefore, the gas-phase acidity of **12b** lies between that of *t*-BuSH and H_2S, and we assign a value of $\Delta_{acid}H_{298}$ = 352 ± 2 kcal/mol. Additional support for this assignment was found by performing the reverse reactions (i.e. the reaction of the 2-oxepinoxy anion (**15a**) with various acids). In that experiment we observed that **15a** underwent proton transfer with H_2S but not with *t*-BuSH, corroborating the results

found for the forward reactions. The experimental gas-phase acidity agrees well with the results of DFT calculations, which provided values of $\Delta_{acid}H_{298} = 348.9$ kcal/mol at the B3LYP/6-31+G(d) level and 349.2 kcal/mol at the B3LYP/aug-cc-pVTZ level. Future measurements on the electron affinity of the 2-oxepinoxy radical and the heat of formation of **12b**, in combination with the experimental data reported here, should lead to the heat of formation of 2-oxepinoxy radical. These studies will give insight to the role that the 2-oxepinoxy radical plays in the oxidation of the phenyl radical.

Acknowledgment. We acknowledge Dr. Ivan Keresztes and Anthony Condo of the Cornell Chemistry NMR facility for help performing and analyzing the 2D NMR experiments. We acknowledge several helpful comments from the reviewers, including the suggestion of the mechanism shown in Scheme 7. C.M.H. acknowledges support from the NSF-funded Environmental Molecular Science Institute (CHE-0089147) and the Ohio Supercomputer Center. B.K.C. acknowledges support of this research by the Department of Energy (Grant DE-FG02-98ER14857). M.P.D. acknowledges a Procter and Gamble fellowship.

Supporting Information Available: ^{13}C NMR, COSY, HSQC, and HMBC spectra; MS data for the reactions of **12b** with anions and **15a** with acids; and Cartesian coordinates, vibrational frequencies, and thermodynamic parameters for stationary points; complete refs 42 and 43. This material is available free of charge via the Internet at http://pubs.acs.org.

JA050173U